Electronic Supplementary Information

Effects of Poly(ethylene glycol) on Wetting Behavior and Director Configuration of Lyotropic Chromonic Liquid Crystals Confined in Cylinders

Hyesong Lee, Vijaya Sunkara, Yoon-Kyoung Cho, and Joonwoo Jeong

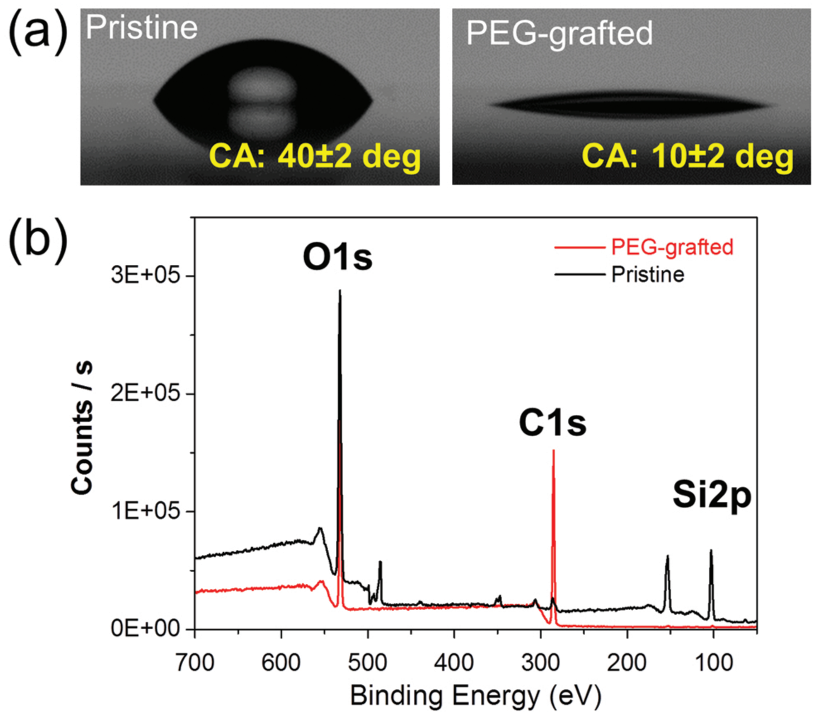

	C1s	O1s	Si2p
Pristine	1.5	63.1	35.4
PEG-grafted	66.3	32.6	1.1

Figure S1: Surface analysis of pristine and PEG-grafted glasses. (a) Representative optical images of sessile deionized water droplets on the glass substrates for the contact angle measurements. (b) X-ray photoelectron spectroscopy results. The table shows the atomic percent (%) of C1s, O1s and Si2p

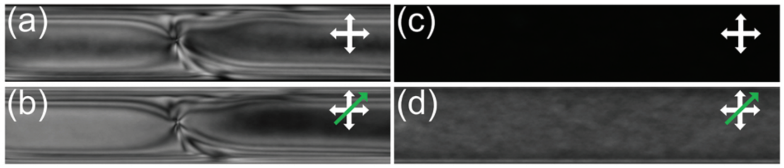

Figure S2: Polarized optical microscopy of 30.0% (wt/wt) nematic SSY in a square capillary with and without PEG under a quasi-monochromatic illumination of wavelength 660 nm. White double arrows represent the pass axes of the linear polarizers, and a green single-headed arrow indicates the slow axis of the full-wave plate (550 nm retardation). (a) and (b) The double-twist director configuration of the neat nematic SSY confined in a square capillary with a 50-μm side. (c) and (d) The parallel-axial director configuration of the PEG-doped nematic SSY in the same square capillary. The concentration of the PEG 35k added is 0.01% (wt/wt).

Comments on the energy difference between the point and domain-wall-like defects

Davidson *et al.* reported that the type of topological defects in the K_{24}-induced DT configuration is determined by the energetics.[1] Fig. S3 shows the comparison of the theoretically estimated energies of two possible defects in the DT director configuration of 30.0% (wt/wt) neat nematic SSY at the room temperature having $K_2/K = 1/10$. It turns out that the nematic SSY has $K_{24}/K \approx 6$, and the point defect has much lower energy than its counterpart by $10^5 k_B T$ when the radius is 25 μm and K is 10 pN. Indeed, in the neat SSY, the domain-wall-like defects have never been reported, while the point defects have not been observed in nematic DSCG of $K_{24}/K \approx 1$ and $K_2/K \approx 1/30$.[2,3] We must note that the theoretical calculations are based on the energy-minimizing director field model of the defects on top of the ideal DT configuration with a planar degenerate anchoring condition. Because it does not provide the energy landscape, no information about the transition pathway between two defects types and the energy barrier is available.

The appearance of the domain-wall-like defects in nematic SSY after PEG doping may hint at the decrease of K_{24}/K down to $\approx$3.5 where the energies of two defect become comparable, but there are significant caveats. First, because the energy calculation in Fig. S3 is based on the ideal DT director configuration with a planar degenerate anchoring, there are no considerations of kinetically trapped meta-stable director configuration and non-degenerate/non-planar surface anchoring. As shown in Movie S1, the PEG doping hinders a relaxation of nematic directors into the DT configuration. We think that this is related to the formation of kinetically-trapped configurations, and we have the experimental observation of the heterogeneity in the POM textures. Additionally, as demonstrated in the first part of the paper, the PEG molecules adsorb to the surface, which may result in the different anchoring than the planar degenerate one. Second, if K_{24}/K can be affected by dopants, other elastics constants may change; Note K stands for $K = K_1 = K_3$ and the energy calculation shown in Fig. S3 are sensitive to the elastic constants.

Comments on the characterization of heterogeneous DT configurations

In contrast to the neat case, the PEG-doped nematic SSY in cylinders exhibit a heterogeneity in its DT configuration. As we discuss in the main text, the doped SSY also has the POM texture of the DT configuration with the topological defects between the domains of different handednesses. However, there exist multiple textures, as shown in Fig. S4 and Fig. 5, while the neat one in Fig. 1 shows only one texture with a well defined twist angle. Because the profile of the transmitted intensity through the central regions of the DT domains directly reflects the director configuration along the beam path, i.e., the twist profile $\beta(r)$, the intensity profiles shown in Fig. S4 confirm the multiple director configuration, even in the same domain of the same handedness.

Our attempts to estimate the twist angles $\beta_1 = \beta(r = R)$ of the heterogeneous DT configuration

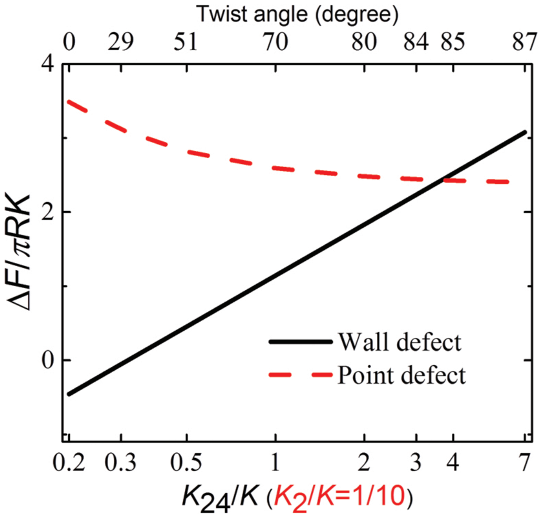

Figure S3: Theoretically estimated energies of the domain-wall-like and point defects relative to the energy of the defect-free double-twist configuration as a function of K_{24}/K with $K_2/K = 1/10$ and $K = K_1 = K_3$ according to Davidson *et al.*[1] The elastic moduli simulate the elastic constants of 30.0% (wt/wt) neat nematic SSY at the room temperature. ΔF stands for the energy difference with the defect-free DT configuration, and R is the radius of the capillary. The top axis shows the twist angle β_1 according to K_{24}/K and eqn S1 in the main text.

of the PEG-doped SSY may hint at the decrease of the twist angle β_1 resulting from the reduction in the saddle-splay elastic modulus K_{24}. However, we must start with a significant caveat in this approach. To characterize the director configuration from experimentally measured optical textures, a director-field *model* is required. We adopt the escaped-twist configuration by the large saddle-splay elastic modulus K_{24} in Davidson *et al.* under the assumption that the elastic constants except the saddle-splay one, are not affected by the doping. Because this characterization indicates that the twist angle β_1 and K_{24} decreases considerably. It seems invalid to assume that the elastic constants hardly get affected by doping. For validation, we need experimental measurements of the director fields and the elastic constants of PEG-doped nematic SSY.

Keeping these caveats in mind, to measure β_1, we first get the intensities of transmitted light through the central region of a DT configuration as a function of the angle between the polarizer and the analyzer. (See Materials and Methods of the main text for details) The intensity profile is compared to the numerically generated profiles to find the best matching β_1 and optical birefringence Δn according to the least square method.[4] Precisely, assuming the escaped-twist director configuration model, we numerically generate transmittance profiles by Jones calculus scanning through a reasonable range for each parameter: Δn and β_1. Then, the least square method find the best candidacies. Finally, we compare the numerically calculated 2D transmittance images with the experimental POM image, and we select one parameter-set having the best image match with the experimental POM image. Note that the estimation of twist angle β_1 from the extrema of the curves is not straightforward. It is because the experimental condition does not lie safely within the waveguiding regime. Additionally, here we fix the polarizer and rotate analyzer, and this method makes intuitive interpretations of the extrema difficult.

This characterization method concludes that $|\beta_1|$ can decrease down to 20 deg by PEG doping from 87 degrees of the neat sample. The solid curves in Fig. S4 are best fits to the data using the Jones calculus: 73 deg for the left part and 24 deg for the right one. The decrease in the twist angle β_1 is directly explained by the PEG-induced reduction of the saddle-splay elastic modulus K_{24}. The twist angle β_1 of the DT configuration in eqn (S1) decreases as the K_{24} decreases.[1] K_2 and K_3 are the twist and bend elastic constants, respectively, and we assume they do not get affected by the doping. It is important to note that, as the varied textures of domains in Figs. 5(a) and S4 indicates, the observed β_1s are quite heterogeneous, mostly ranging from 20 to 80 degrees.

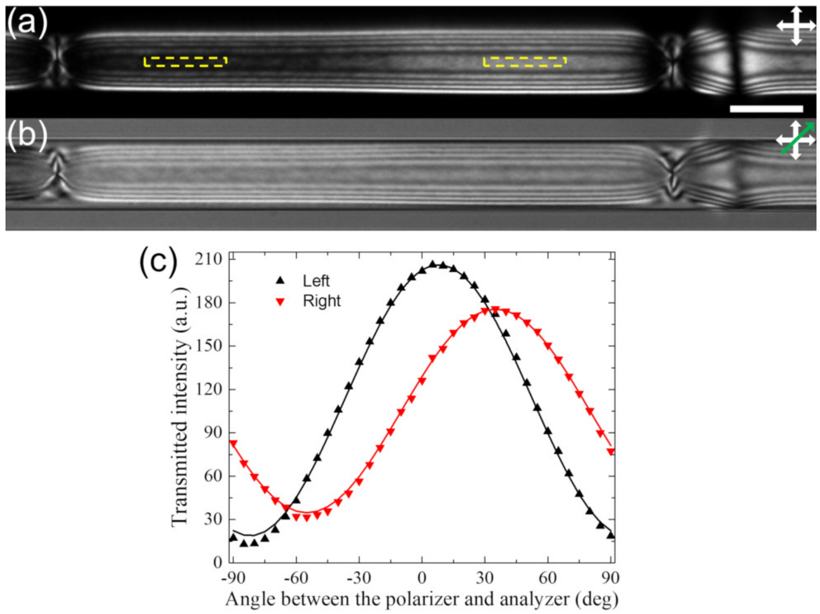

Figure S4: Double-twist (DT) director configuration of nematic SSY confined in cylindrical cavities and the profiles of transmitted light intensities through the central region. (a) and (b) POM images of the DT director configuration of PEG-doped 30.0% (wt/wt) nematic SSY between crossed polarizers (a) without and (b) with a full-wave plate (550 nm retardation) under a quasi-monochromatic illumination of wavelength 660 nm. The concentration of the 35k PEG added is 0.01% (wt/wt). White double arrows represent the pass axes of the linear polarizers and a green single-headed arrow indicates the slow axis of the full-wave plate. Scale bar: 50 μm. Note that the regions highlighted by yellow boxes have different brightness even though they are in the same domain of the same handeness. (c) The profiles of the transmitted light intensities through the yellow boxes in (a) as a function of the angle between the polarizer and the analyzer. The solid curves are the best fits. (See the text for the details of the fitting.)

$$\beta(r) = \arctan \frac{2\sqrt{K_2 K_{24}(K_{24} - 2K_2)}r/R}{\sqrt{K_3}[K_{24} - (K_{24} - 2K_2)r^2/R^2]},$$
$$\beta(r/R) = \beta_1 = \arctan \sqrt{\frac{K_{24}(K_{24} - 2K_2)}{K_2 K_3}}. \tag{S1}$$

To our interest, the decrease of $|\beta_1|$ and K_{24} in this characterization is qualitatively consistent with the following experimental observations. First, the PEG-doped SSY in square capillaries often exhibits the parallel-axial configuration with no twist while the neat SSY shows the DT configuration in the same square capillaries.[5] As shown in Fig. S2, the square capillary with the PEG-doped SSY looks dark when the crossed polarizers are aligned parallel and perpendicular to the capillary axis, respectively. Considering that the DT configuration in the square capillary also results from the large K_{24},[5] the observed parallel-axial director configuration is consistent with the reduction of K_{24} and $|\beta_1|$. Second, the appearance of the domain-wall-like defect in Fig. 5(a) is also consistent with the decreased K_{24} scenario.[1] The neat SSY of $K_{24}/K_3 \approx 6$ shows only a point defect between two domains of different handedness because the point defect has several times lower energy than the domain-wall-like defect when $K_{24}/K_3 = 6$ in Fig. S3. Note that energies of two different types of defects become comparable when $K_{24}/K_3 \approx 3.5$, and we expect to observe two types of defects of comparable energies with similar probabilities, as observed in our PEG-doped SSY case.

Further calculations do not support the PEG-induced reduction of K_{24}. To explain the decrease of β_1 after the PEG doping, K_{24}/K_3 should decrease from 6 to 0.3 according to eqn (S1) under the assumption that the doping does not affect the other elastic constants, i.e., twist and bend constants. We think this 20-fold decrease is not feasible considering the minuscule amount of PEG added, i.e., 0.01% (wt/wt). Additionally, this scenario of K_{24} reduction can not explain the heterogeneity in the director configurations and the resulting textures. Lastly, if K_{24}/K_3 decrease from 6 to 0.3, domain-wall-like defects should dominantly appear because they have much lower energy than the point defect as shown in Fig. S3. However, we observe both types of defects in experiments, with inconsistent number ratios in each experimental trial. These are why we mainly present in the main text the hypothesis about the formation of the meta-stable director configuration.

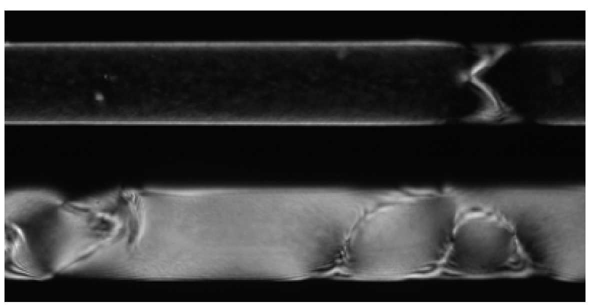

Movie S1: A movie of isotropic-to-nematic phase transition in 30.0% (wt/wt) SSY in cylindrical capillaries of 100-μm diameter. (Top) Neat SSY (Bottom) With 0.01% (wt/wt) 35k PEG. The samples are placed between two crossed polarizers aligned along North-to-South and West-to-East, respectively. The movie is ten times sped up.

---

[1] Z. S. Davidson, L. Kang, J. Jeong, T. Still, P. J. Collings, T. C. Lubensky and A. G. Yodh, *Physical Review E*, 2015, **91**, 1–5.

[2] S. Zhou, K. Neupane, Y. A. Nastishin, A. R. Baldwin, S. V. Shiyanovskii, O. D. Lavrentovich and S. Sprunt, *Soft Matter*, 2014, **10**, 6571–81.

[3] K. Nayani, R. Chang, J. Fu, P. W. Ellis, A. Fernandez-Nieves, J. O. Park and M. Srinivasarao, *Nature Communications*, 2015, **6**, 8067.

[4] A. Javadi, J. Eun and J. Jeong, *Soft Matter*, 2018, **14**, 9005–9011.

[5] J. Fu, K. Nayani, J. O. Park and M. Srinivasarao, *NPG Asia Materials*, 2017, **9**, e393.